# Hysteresis Modeling and Compensation of PZT Milliactuator in Hard Disk Drives

Zhen Zhang
School of Automation Science and Electrical Engineering
Beijing University of Aeronautics and Astronautics
Beijing, China, 100191
Email: zhangzhen@buaa.edu.cn

Chunling Du, Tingting Gao
A*STAR, Data Storage Institute
Singapore, 117608
Email: DU_Chunling@dsi.a-star.edu.sg;

Lihua Xie
School of Electrical and Electronic Engineering
Nanyang Technological University
Nanyang Avenue, Singapore 639798
Email: elhxie@ntu.edu.sg

***Abstract*—Dual-stage actuation consisting of a PZT Microactuator (MA) and a Voice Coil Motor (VCM) has been used to improve the servo bandwidth and the disturbance rejections of Hard Disk Drivers (HDDs). However, the hysteresis in PZT MA limits the performance that can be achieved. In this paper, a Hammerstein model structure consisting of static hysteresis nonlinear block and dynamic linear block is used to model the PZT MA in HDDs and the identification method is also given. The nonlinear subsystem in the Hammerstein model is represented by Modified Prandtl-Ishlinskii (MPI) hysteresis model. It is proved that the proposed model is equivalent to the physical system. A hysteresis compensator is designed based on the proposed model. By the hysteresis compensation, the effects of hysteresis on the frequency responses of the PZT MA are measured. It is shown that apparent phase lead is achieved by hysteresis compensation, which is useful to improve the performance of control system.**

***Keywords*—hysteresis, modeling, Hammerstein, PZT, Hard Disk Drivers**

## I. INTRODUCTION

The dual-stage actuation system consisting of a voice motor (VCM) and a PZT microactuator has been proposed as an effective way to attain a high servo bandwidth and achieve required disturbance and runout rejections in HDDs [1][3]. In a dual-stage actuation system, the VCM actuators is used as the primary stage to provide large but relatively slow movement while the secondary stage PZT microactuator is used to provide fine and fast positioning. In the secondary stage, the PZT suspension utilizes two PZT elements which expand and contract in their lengthwise directions when a voltage potential is applied across their thickness. Recently, many dual-stage control design methodologies have been developed, including sensitivity decoupling control [1], PQ method [2] and those based on modern optimal control design method (such as LQG[4], $H_\infty$ control[5], μ-synthesis [6], mixed $H_2/H_\infty$ control [7].

However, hysteresis nonlinearity is an inherent characteristic of the PZT material, which decreases the performance of the control system and even results in limit cycle oscillations [8]. 'Rate-independent memory effects' was used as a general hysteresis definition [9]. For the hysteresis system, the output of the system depends not only on the present input, but also on the past input (memory). Rate-independent means that input-output relationship is invariant with respects to changes in time scales. The basic idea to deal with the hysteresis is inverse compensation by constructing a right inverse of hysteresis model. Most of feedback controller designs for dual-stage system in HDDs did not account for the hysteresis effects from PZT material. In [10], GPI model is used to model the hysteresis of the PZT MA in HDDs and the inverse of the GPI is used as the hysteresis compensator.

The challenges of controller design for PZT suspension in HDDs considering hysteresis effects in PZT element are the modeling of the PZT suspension. The hysteresis model due to the PZT element in HDDs should be identified to design the inverse compensator, and the dynamic response of the suspension structure removing the hysteresis effects should be also measured and identified to design the servo controller, while it is difficult to identify them directly because the internal state between the PZT element and the suspension structure is unmeasurable.

These motivate the present work concerning on the modeling of the hysteresis in the PZT MA in HDDs, analysis of the hysteresis effects on the frequency response of the system and compensating it. An equivalent block-oriented hysteresis model for the PZT MA is presented and the identification method is also given. The novel hysteresis model with Hammerstein model structure has the same input-output relationship with the physical system but the subsystems in it do not correspond to physical components in the PZT MA. The hysteresis block in the proposed model is based on the Modified Prandtl-Ishlinskii (MPI) hysteresis model [8]. Compared with other hysteresis model such as Preisach model [11] [12], Prandtl-Ishlinskii model [13], Bouc-Wen model [15] and Duhem model [14], MPI model has advantages of computational simplicity, analytical inverse and asymmetric hysteresis loops, which is attractive to real-time control. Based on the proposed hysteresis model of the PZT MA, a hysteresis compensator is designed and the effects of the hysteresis on the frequency response of the PZT suspension are shown experimentally. The main contribution of this paper is the hysteresis modeling of the PZT suspension. A linear system can be identified by cascading the inverse compensator with the PZT MA and it can be seen that there is remarkable phase-lead in frequency response by using inverse compensator, which is important to servo controller design.

The remainder of the paper is organized as follows. Section II introduces the MPI model and its analytical inverse briefly. Section III presents the hysteresis model of the PZT suspension and identification method. Section IV presents the hysteresis compensation results and the effects of compensation on the frequency response of the PZT MA. Finally, Section V concludes the paper.

## II. MODELING OF HYSTERESIS

In this section threshold-discrete MPI model and its inversion are given briefly. The detailed description of MPI model can be found in [8].

### A. Prandtl-Ishlinskii (PI) Model

The elementary operator in the PI hysteresis is the so-called play or backlash operator shown in Fig. 1, which is defined as

$$H_r [x, y_0] (t)=\max \{x(t)-r, \min \{x(t) + r, y\}\} \quad (1)$$

for piecewise monotone continuous input signal with a monotonic partition $0=t_0 \leq t_1 \leq \ldots \leq t_N = t_E$. The operator is characterized by its threshold $r \in \Re_+$. The initial consistency condition of (1) can is given as

$$H_r[x, y_0](0) = \max\left\{x(0)-r, \min\left\{x(0)+r, y_0\right\}\right\} \quad (2)$$

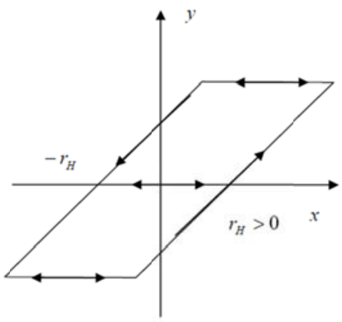


Figure. 1 Characteristic of the play operator

with $y_0 \in \Re$, which is usually but no necessarily initialized to zero.

So the output of so-called the threshold-discrete Prandtl-Ishlinskii hysteresis operator is defined as

$$y(t) = \mathbf{w}_\mathbf{H}^\mathbf{T} \cdot \mathbf{H}_{\mathbf{r}_\mathbf{H}}[x, \mathbf{y_0}](t) \quad (3)$$

with weight vector $\mathbf{w}_\mathbf{h}^\mathbf{T} = [w_{h0} \ldots w_{hn}]$, the threshold vector $\mathbf{r}_h = [r_{h0} \ldots r_{hn}]^T$ with $0 = r_{h0} < r_{h1} < \ldots < r_{hn} < +\infty$, the vector of the initial states $\mathbf{y_0} = [y_{00} \ldots y_{0n}]^T$ and the vector of the play $\mathbf{H}_\mathbf{r}[x, \mathbf{y_0}](t) = [H_{r_{h0}}[x, y_{00}](t) \ldots H_{r_{hn}}[x, y_{0n}](t)]^T$.

### B. Modified Prandtl-Ishlinskii Model

The closed loops of PI operator have an odd symmetry property to the center point of the corresponding loop. The fact that most real actuator hysteresis loops are not symmetric reduces its applicability in practice. To overcome this overly restrictive property, a modified Prandtl-Ishlinskii hysteresis modeling approach has been developed by combining a so-called Prandtl-Ishlinskii superposition operator (PISO) in series with the PI operator. PISO is a weighted linear superposition of one-sided dead zone operators. For threshold $r_s \in \Re$, a dead zone operator is defined as

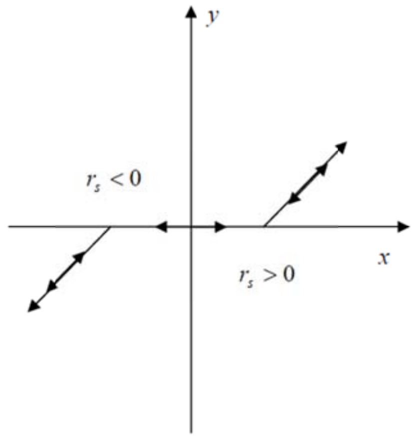


Figure. 2 Characteristic of the one-sided deadzone operator

$$S(x(t), r_s) = \begin{cases} \max\left\{x(t) - r_s, 0\right\}; & r_s > 0 \\ x(t) & ; \ r_s = 0 \\ \min\left\{x(t) - r_s, 0\right\}; & r_s < 0 \end{cases} \quad (4)$$

This elementary superposition operator is also fully characterized by a threshold parameter $r_s \in \Re$. Fig. 2 shows the output-input trajectory of this elementary superposition operator for different threshold values. The complex superposition operator for the approximation of more general continuous memory-free nonlinearities is given by

$$S[x](t) = \mathbf{w_s}^\mathbf{T} \cdot \mathbf{S}_{\mathbf{r}_s}[x](t) \quad (5)$$

with the vector of weights $\mathbf{w_s}^\mathbf{T} = (w_{s-l} \ldots w_{s0} \ldots w_{sl})$, the vector of thresholds $\mathbf{r_s}^\mathbf{T} = (r_{s-l} \ldots r_{s0} \ldots r_{sl})$ with $-\infty < r_{s-l} < \ldots < r_{s0} = 0 < \ldots < r_{sl} < +\infty$ and the vector of the one-sided dead-zone operators $\mathbf{S_r}^\mathbf{T} = (S_{r_{s-l}} \ldots S_{r_{s0}} \ldots S_{r_{sl}})$. The modified PI operator is thus

$$y(t) = \Gamma[x](t) = \mathbf{w_s}^\mathbf{T} \cdot \mathbf{S}_{\mathbf{r}_s}[\mathbf{w_H}^\mathbf{T} \cdot \mathbf{H}_{\mathbf{r}_\mathbf{H}}[x, \mathbf{y_0}]](t) \quad (6)$$

with $\mathbf{r_H} \in \Re_+^{\mathbf{n+1}}$, $\mathbf{w_H} \in \Re^{\mathbf{n+1}}$, $\mathbf{r_S} \in \Re^{\mathbf{2l+1}}$, $\mathbf{w_S} \in \Re^{\mathbf{2l+1}}$

In MPI model formulated by (6), parameters $\mathbf{r_s}$, $\mathbf{r}_h$, $\mathbf{w_s}$, $\mathbf{w_h}$ should be determined. The identification method can be found in [16], which is formulated as a quadratic optimization problem with linear inequality and equality constraints and a least square scheme is employed to identify them.

*C. Inversion of MPI*

For (6), if there exists $\varepsilon > 0$ let

$$\begin{Bmatrix} \mathbf{U_H} & \\ & \mathbf{U}_S \end{Bmatrix} \cdot \begin{Bmatrix} \mathbf{w_H} \\ \mathbf{w_S} \end{Bmatrix} \ge \begin{Bmatrix} \mathbf{u_H} \\ \mathbf{u_S} \end{Bmatrix}, \tag{7}$$

where $\mathbf{U_H} = \begin{bmatrix} 1 & 0 & \cdot & 0 \\ 0 & 1 & \cdot & 0 \\ \cdot & \cdot & \cdot & \cdot \\ 0 & 0 & \cdot & 1 \end{bmatrix} \in \Re^{\mathbf{n+1 \times n+1}}$ , $\mathbf{u_H} = \begin{bmatrix} \varepsilon \\ 0 \\ 0 \\ 0 \end{bmatrix} \in \Re^{\mathbf{n+1}}$ ,

$$\mathbf{U_s} = \begin{bmatrix} 1 & \cdots & 1 & 1 & 0 & \cdots & 0 \\ \vdots & \ddots & \vdots & \vdots & \vdots & \therefore & \vdots \\ 0 & \cdots & 1 & 1 & \cdots & \cdots & 0 \\ 0 & \cdots & 0 & 1 & \cdots & \cdots & 0 \\ 0 & \cdots & 0 & 1 & 1 & \cdots & 0 \\ \vdots & \therefore & \vdots & \vdots & \vdots & \ddots & \vdots \\ 0 & 0 & 0 & 1 & 1 & \cdots & 1 \end{bmatrix} \in \Re^{\mathbf{2l+1 \times 2l+1}}, \quad \mathbf{u_s} = \begin{bmatrix} \varepsilon \\ \vdots \\ \varepsilon \\ \varepsilon \\ \varepsilon \\ \vdots \\ \varepsilon \end{bmatrix} \in \Re^{\mathbf{2l+1}},$$

then the inverse model of MPI exists uniquely as

$$\Gamma^{-1}[y](t) = \mathbf{w_H^{'T}} \cdot \mathbf{H}_{\mathbf{r_H^{'}}}[\mathbf{w_S^{'T}} \cdot \mathbf{S}_{\mathbf{r_S^{'}}}[y], \mathbf{y_0^{'}}](t) \tag{8}$$

with $\mathbf{r_H^{'}} \in \Re_+^{\mathbf{n+1}}$ , $\mathbf{r_S^{'}} \in \Re^{\mathbf{2l+1}}$ , $\mathbf{w_S^{'}} \in \Re^{\mathbf{2l+1}}$ , $\mathbf{w_H^{'}} \in \Re^{\mathbf{n+1}}$ , $\mathbf{y_0^{'}} \in \Re^{\mathbf{n+1}}$.

So the thresholds, the weights and the initial states of the models and their corresponding inverse exist one to one correspondence. The detailed transformation laws between them can be expressed as

$$r_{hi}^{'} = \sum_{j=0}^{i} w_{hj}(r_{hi} - r_{hj}); \quad i = 0 \ldots n \tag{9}$$

$$w_{h0}^{'} = \frac{1}{w_{h0}},$$

$$w_{hi}^{'} = -\frac{w_{hi}}{(w_{h0} + \sum_{j=1}^{i} w_{hj})(w_{h0} + \sum_{j=1}^{i-1} w_{hj})}; i = 1 \ldots n \tag{10}$$

$$y_{0i}^{'} = \sum_{j=0}^{i} w_j y_{0i} + \sum_{j=i+1}^{n} w_j y_{0j} \quad ; \quad i = 0 \ldots n \tag{11}$$

$r_s \in \Re^+$,

$$r_{si}^{'} = \sum_{j=0}^{i} w_{sj}(r_{si} - r_{sj}) \quad ; i = 0 \ldots l \tag{12}$$

$$w_{si}^{'} = -\frac{w_{si}}{(w_{s0} + \sum_{j=1}^{i} w_{sj})(w_{s0} + \sum_{j=1}^{i-1} w_{sj})}; i = 1 \ldots l \tag{13}$$

$r_s \in \Re^-$,

$$r_{si}^{'} = \sum_{j=i}^{0} w_{sj}(r_{si} - r_{sj}) \quad ; i = -l \ldots 0 \tag{14}$$

$$w_{s0}^{'} = \frac{1}{w_{s0}}$$

$$w_{si}^{'} = -\frac{w_{si}}{(w_{s0} + \sum_{j=i}^{-1} w_{sj})(w_{s0} + \sum_{j=i+1}^{-1} w_{sj})}; i = -l \ldots -1 \tag{15}$$

## III. HYSTERESIS MODELING OF PZT SUSPENSION AND ITS INVERSE COMPENSATION

*A. The PZT suspension model*

The PZT suspension is a dynamic nonlinear system and can be described by Fig. 3, where $H$ represents the hysteresis nonlinearity of the PZT elements, $G_M$ indicates the dynamic response of suspension structure and is a LTI system. $H$ and $G_M$, corresponding to physical components in the PZT suspension, should be identified experimentally in order to design the inverse compensator and feedback servo controller.

Unfortunately it is difficult to identify them directly because the internal state $x = H[u](t)$ is unmeasurable. A block-oriented model is proposed for the PZT suspension shown in Fig. 4. The model is of Hammerstein model structure, in which $H^*$ presents a hysteresis nonlinear subsystem and $G_M^*$ presents a LTI subsystem. The subsystems in the Fig. 4 do not correspond to the physical component in the PZT suspension. An identification method of the proposed Hammerstein model is designed. By the identification method the proposed model is equivalent to the physical system of the PZT suspension. The identification method is given as follow:

Step 1 A quasi-static excitation signal $u$ is applied to the PZT suspension, and then the output of the PZT suspension $v$ is measured.

Step 2 From the measured data ($u$, $v$), the subsystem $H^*$ is modeled using MPI hysteresis model. The hysteresis compensator $H^{*-1}$ is designed based on the inverse of the subsystem $H^*$ using (9)-(15).

Step 3 By cascading the inverse compensator $H^{*-1}$ with the PZT suspension shown in Fig. 5, the frequency response of subsystem $G_M^*$ can be measured and identified.

It can be proved that by the identification method the proposed Hammerstein model has the same input-output relationship as the physical system of the PZT suspension shown in Fig. 3.

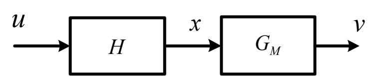


Figure. 3 Model Structure of the PZT suspension

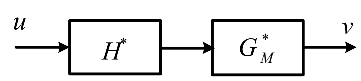


Fig. 4 Hammerstein system of the PZT suspension

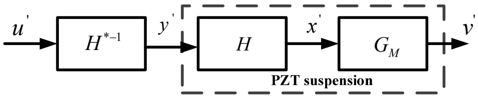


Figure. 5 Identification of the LTI subsystem

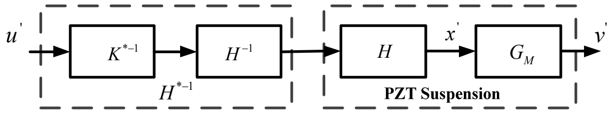


Figure. 6 Inverse of the hysteresis in Hammerstein model

Let $G_M = K^* G_M^*$ where $K^*$ is the gain of the subsystem $G_M$ and $H^* = K^* H$, then the system in Fig. 4 is equivalent to the physical system shown in Fig. 3. So it should be proved that the subsystems $G_M^*$, $H^*$ can be identified by the proposed identification method.

**Proof:** Under a quasi-static excitation signal $u$, the output of the PZT suspension $v$ can be approximated as $v(t) = K^* H[u](t)$. So the block $H^* = K^* H$ can be identified from measured data ($u$, $v$). The hysteresis inverse compensator $H^{*-1}$ is gotten and used to cancel the hysteresis effects in the PZT suspension as shown in Fig. 6. The internal state $x^{'}(t) = u^{'}(t) / K^*$. The s-domain output of $v^{'}$ is $V^{'}(s) = G_M(s) U^{'}(s) / K^*$, with $G_M = K^* G_M^*$, $V^{'}(s) = G_M^*(s) U^{'}(s)$. So the block $G_M^* = G_M / K^*$ can be identified from the input-output data $(u^{'}, v^{'})$.

**Remark**: In order to improve the bandwidth of the servo system, the mechanical structure of the PZT suspension is designed with high resonance frequency, so the frequency response of the PZT suspension can be approximated as a gain at the low frequency range, which is about 1 kHz in this PZT suspension.

### *B. Modeling results of the PZT suspension*

The HDD used in modeling experiment has all its cover and disk plates removed and is placed on a vibration-free platform. A laser Doppler vibrometer (LDV) is used to measure the position of the dual-stage actuator, the resolution used is 100nm/V. The controllers are implemented with dSPACE 1103 on TMS320C240 DSP board. A Dynamical signal analyzer (DSA) is used to measure the frequency response of the system. The sampling frequency is 40 kHz.

In order to identify the hysteresis subsystem $H^*$ in the proposed model, the sinusoidal waves are used to excite the PZT suspension. The responses and the input-output relationship of the PZT suspension at 0.5K frequency excitation signal are given in the Fig. 7 and Fig. 8 respectively. It can be seen that there are remarkable low-frequency displacement drift and high-frequency noise in the measurement, which causes the identification difficult. The output of the hysteresis system is periodic signal under periodic input. So the band-pass filters are used to filter out the effects of low-frequency drifts and high-frequency noise in measurement. Fig. 9 gives the filtered experimental results of the hysteresis loops under 0.5k, 0.8k and 1k frequency excitation signals. It is shown that there are only minor differences among the hysteresis loops under different input signals below 1K frequency. The experimental data under 0.8K frequency input signal is used to identify the subsystem $H^*$. Fig. 10 gives the comparisons between the hysteresis modeling results by MPI and the experimental data with and without band-pass filter. Good agreements are shown between the model simulation results and the experimental data.

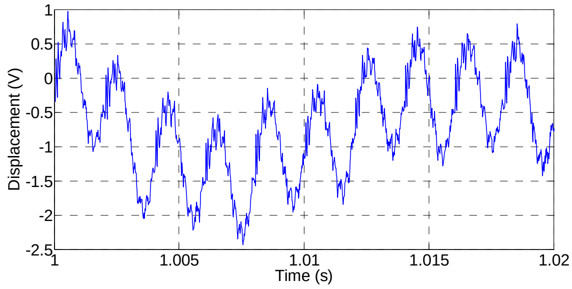


Figure. 7 Responses of the PZT suspension

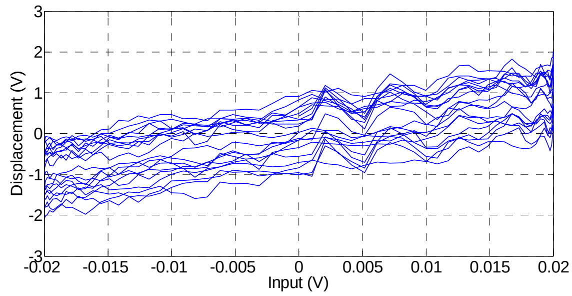


Figure. 8 Input-output relationship of the PZT suspension

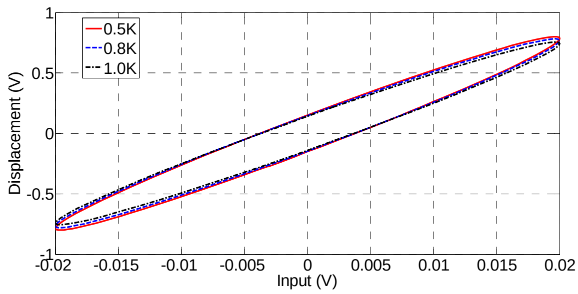


Fig. 9 Hysteresis loops under different input signals

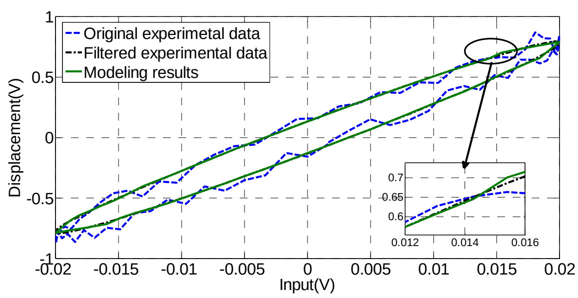


Figure. 10 Modeling results of the hysteresis loops

From the identified $H^*$, the inverse compensator $H^{*-1}$ is designed and used to cancel the hysteresis effects in the PZT suspension as shown in Fig. 5. The input signal is sinusoidal wave with 0.8 k Hz frequency. The responses of the open loop hysteresis compensation system are given in the Fig. 11 and obvious displacement drift and noise can be also observed. Fig. 12 gives the plots of measured input signal against output signal. It is shown in Fig. 12 that the hysteresis behaviors are reduced significantly by the hysteresis compensator. The system consisting of the hysteresis compensator and the PZT MA is approximately linear.

Then the frequency response of LTI subsystem $G_M^*$ are measured by DSA using swept sine input signal and shown in Fig. 13. In order to demonstrate the effects of the hysteresis on the frequency response of the PZT MA, the measured frequency response of the PZT MA without inverse compensator is also given in Fig. 13. It is shown in Fig. 13 that apparent 'phase-lead' and 'gain shift' can be observed by using the inverse compensation. It is because that the hysteresis subsystem in the suspension system plays a role as 'phase lag' depending on the amplitude of the input and more generally on past input extrema, but not on frequency as linear system. In frequency domain controller design, the phase lag in open loop transfer function will cause decrease of phase margin, so the inverse compensation of hysteresis will increase frequency domain performances such as phase margin and bandwidth.

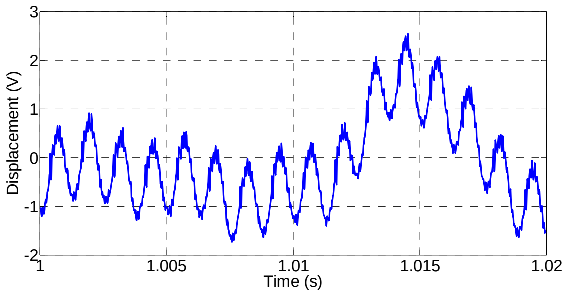


Fig. 11 Output displacement of the open loop compensation

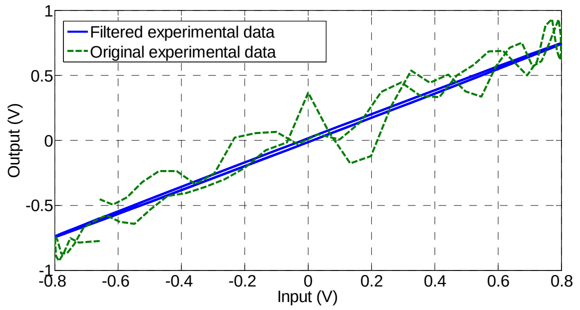


Figure. 12 Input-output relationship of open loop hysteresis compensation

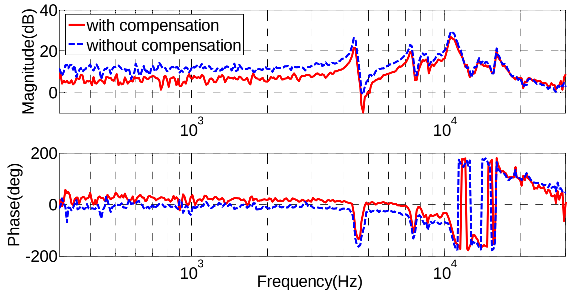


Figure. 13 Comparison of frequency response between with and without hysteresis compensation

## IV. CONCLUSION

A block-oriented dynamic hysteresis nonlinear model for the PZT suspension in the dual-stage system of HDD is proposed, which is equivalent to the physical system. Based on the proposed model the inverse compensator is designed. Experimental results show that the inverse compensator is effective for compensating the hysteresis effects in PZT MA. A linear system is measured by cascading the compensator with the PZT suspension. Comparisons of the frequency responses of the PZT suspension with and without compensator shown that the remarkable phase lead is achieved by hysteresis compensation, which is attractive to improve the phase margin and the bandwidth of the servo control system of HDDs.

## REFERENCES


[1] Y. Li and R. Horowitz, "Mechatronics of electrostatic microactuators for computer disk drive dual-stage servo systems," IEEE/ASME Trans. Mechatronics, vol. 6, no. 2, pp. 111–121, 2001.

[2] S. Schroeck, W. Messner, and R. McNab, "On compensator design for linear time-invariant dual-input single-output systems," IEEE/ASME Transactions on Mechatronics, vol.6, no. 1, pp. 50-57, 2001.

[3] Kemao Peng, Ben M. Chen, Tong H. Lee, V. Venkataramanan, "Design and implementation of a dual-stage actuated HDD servo system via composite nonlinear control approach," Mechatronics, vol. 14, no. 9, pp. 965-988, 2004.

[4] X. P. Hu, W. Guo, T. Huang and B. M. Chen, "Discrete-time LQG/LTR dual-stage controller design and implementation for high track density HDDs," presented at American Control Conference, San Diego, USA, pp. 4111 – 4115, 1999.

[5] Chunling Du, Guoxiao Guo, "Lowering the hump of sensitivity functions for discrete-time dual-stage systems," IEEE Transactions on Control Systems Technology, vol. 13, no. 5, pp. 791 – 797, 2005.

[6] X. Huang, R. Nagamune, and R. Horowitz, "A comparison of multirate robust track-following control synthesis techniques for dual-stage and multi-sensing servo system in hard disk drives," IEEE Transactions On Magnetics, vol. 42, no. 7, pp. 1896-1904, 2006.

[7] D. Shim, H. Lee, and L. Guo, "Mixed-objective optimization of track-following controllers using linear matrix inequalities," presented at American Control Conference, 4323-4328, 2003.

[8] K. Kuhnen, "Modeling, identification and compensation of complex hysteretic nonlinearities - a modified Prandtl-Ishlinskii approach," European Journal of Control, vol. 9, no. 4, pp. 407-418, 2003.

[9] A. Visintin, Differential Models of Hysteresis. Springer-Verlag, New York, 1994, pp. 12-13.

[10] Yan Zhi Tan, Chee Khiang Pang, Fan Hong, Sangchul Won, and Tong Heng Lee, "Hysteresis Compensation of Piezoelectric Actuators in Dual-Stage Hard Disk Drives," presented at Proceedings of 2011 8th Asian Control Conference, Kaohsiung, Taiwan, 1024-1029, 2011.

[11] A. Cavallo, C. Natale, S. Pirozzi, and C. Visone, "Effects of Hysteresis Compensation in Feedback Control Systems," presented at IEEE Trans. Magn., vol. 39, no. 3, pp. 1389‑1392, May 2003.

[12] I. D. Mayergoyz, Mathematical Models of Hysteresis. Springer-Verlag, New York, 1991.

[13] M. Rakotondrabe, "Classical Prandtl-Ishlinskii modeling and inverse multiplicative structure to compensate hysteresis in piezoactuators," presented at American Control Conference, Montreal, pp. 1646 - 1651 2012.

[14] J. Oh and D. S. Bernstein, "Semilinear Duhem model for rateindependent and rate-dependent hysteresis," IEEE Transactions on Automatic Control, vol. 50, no. 5, pp. 631‑645, 2005.

[15] Fayçal Ikhouane, José Rodella, "Systems with Hysteresis: Analysis, Identification and Control Using the Bouc-Wen Model," John Wiley &Sons, England, 2007.

[16] Z. Zhang, J. Q. Mao, W. L. Chen. "Stress-Dependent Hysteresis Modeling and Tracking Control of Giant Magnetostrictive Actuator for Periodic Reference Input," presented at Proceedings of the 17th IFAC, Seoul, pp. 2288-2293, 2008.

[17] J. M. Cruz-Hernández, V. Hayward, "Phase Control Approach to Hysteresis Reduction," IEEE Transactions on Control Systems Technology, vol. 9, no. 1, pp. 17-26, January, 2001.

[18] M. Nordin, X. Ma, and P.O. Gutman, "Controlling mechanical systems with backlash: a survey," Automatica, 38:1633–1649, 2002.

[19] M. Stuebner, J. Atulasimha and R. C. Smith, "Quantification of hysteresis and nonlinear effects on the frequency response of ferroelectric and ferromagnetic materials," Smart Mater. Struct., 18(10), pp. 1-10 2009